Supporting information for Manuscript *ac-2009-00465w.R1*

We have measured association and dissociation curves of 7 specific mouse antibodies against 7 small-molecule drugs by conjugating the drugs to BSA and PVA and using the latter to immobilize the drug targets to epoxy-coated glass surfaces. From the binding curves, we obtained the equilibrium dissociation constants for these antibodies against their drug targets.

1. Binding reactions of anti-DNP (2,4-dinitrophenol) goat whole IgG with DNP-BSA and DNP-PVA conjugates

Materials. PVA (average M_w = 89,000 - 98,000 daltons, > 99% hydrolyzed) were purchased from Sigma Aldrich (St. Louis, MO). Sodium hydride (60% dispersion in mineral oil), epichlorohydrin, ammonium hydroxide and 1-fluoro-2,4-dinitrobenzene were purchased from Sigma Aldrich (St. Louis, MO). The reagents were used as received.

Preparation of amine-modified PVA. PVA were modified with amino groups in three chemical steps as shown in Fig. 1: (1) treatment with sodium hydride (NaH) in dry DMSO to deprotonate a prescribed fraction of hydroxyl groups on PVA; (2) reaction with 10-fold excess epichlorohydrin (a Williamson reaction) to add epoxy groups at deprotonated hydroxyl groups; (3) reaction with an ammonium hydroxide aqueous solution to simultaneously open the epoxy rings and add amino groups. The details are as follows. Under N_2 atmosphere and at room temperature, 100 mL of 2 vol. % polyvinyl alcohol in dry DMSO was mixed with a prescribed amount of sodium hydride (NaH, in mineral oil). The amount of NaH was determined by the molar percentage of NaH to available hydroxyl groups on unmodified PVA so that the same molar percentage of hydroxyl groups on PVA (i.e., loading) would be modified with primary amino groups. The actual "loading" of amine groups (i.e., the amount of conjugated amino groups relative to the original hydroxyl groups) on the PVA was quantified by ^{1}H NMR and

elemental analysis. For example to modify 10% of hydroxyl groups on a PVA with amine groups, we make a mixture of NaH in mineral oil at 60% by weight. We then add 100 mL of 2 vol.% PVA in DMSO to 186 mg of the NaH-mineral oil mixture (with 110 mg or 4.6 mmol of NaH in it) to yield a 10% molar ratio of NaH to hydroxyl groups (i.e., 0.10 equ.). The mixture was stirred for 2 hours, then epichlorohydrin (C_3H_5OCl, 0.5 equ. 23 mmol, 2.1 g) was added, and the new mixture was agitated overnight. Afterward 30 mL of 28% aqueous ammonium hydroxide solution was added to the mixture and stirred under N_2 atmosphere for 24 hours. Subsequently, ethanol (5 times in volume) was added to the mixture to precipitate amine-derivatized PVA. The amine-modified PVA was washed with ethanol until the washing filtrate showed negative in Kaiser Test. The polymer was further washed 3 times with acetonitrile, then dissolved in 20 mL of pure water, and finally lyophilized to yield white powders.

The loading of conjugated amino groups on an amine-modified PVA was analyzed by nitrogen elemental analysis as shown in Table 1. The elemental analysis confirmed that the molar percentage of amine-substituted hydroxyl groups was close to the molar percentage of added base NaH (base), especially for PVA with M.W. = 13 kDa and 89 kDa and over 98% hydrolyzed. For PVA with M.W. = 2 kDa and only 75% hydrolyzed, we found consistent lower-than-expected derivatization. This was due to the presence of acetyl groups (25%) on the PVA which consumed some of added NaH. In Fig. 2, we show the ^1H NMR spectra of PVA in DMSO. Compared to unmodified PVA, 4 new peaks appeared in the spectrum of the epoxy-PVA: the ether protons (H_a and H_b) at 3.37 and 3.30 ppm, and protons (H_c, H_d and H_e) on epoxy ring at 2.73 to 2.89 ppm. After the treatment with aqueous ammonium hydroxide, the epoxy rings were opened up and the peaks of epoxy protons disappeared; at the same time two new peaks emerged in the spectrum of amine-modified PVA: ether protons (H_f) around 3.63 ppm and amino-neighboring protons (H_g) at 2.76 ppm; the peak of hydroxyl-neighboring protons

merged with the peak of the PVA backbone at 3.75 ~ 4.00 ppm.

Conjugation of 2,4-dinitrophenol (DNP) to amine-modified PVA. We conjugated DNP to PVA by starting with 2,4-dinitrobenzene molecules (the key part of 2,4-dinitrophenol) and reacting the 10% amine-derived PVA with 1-fluoro-2,4-dinitrobenzene in DMSO under a basic condition (0.1 M $NaHCO_3$). The loading of DNP (0.75% and 1.5% in our present study) was controlled by the molar percentage of 1-fluoro-2,4-dinitrobenzene in the reaction mixture to hydroxyl groups on the original PVA. After the reaction, DNP-PVA conjugates were precipitated and purified using the same method for biotin-PVA conjugates.

Conjugation of DNP to BSA. We used the same chemical steps as for amine-modified PVA to add DNP to BSA by adding a suitable amount of NHS ester of biotin or 1-fluoro-2,4-dinitrobenzene to 5 mL of BSA (2 mg/mL) in 0.1 M $NaHCO_3$ and agitating the mixture overnight at 4°C. DNP-BSA conjugates was precipitated with addition of 25 mL of ethanol to the mixture and then purified accordingly. The loading of DNP was specified by the molar ratio of 1-fluoro-2,4-dinitrobenzene to BSA which was chosen to be 5, 10, 20, and 40 in our present study.

Preparation of small molecule microarrays. DNP-BSA and DNP-PVA were dissolved in 1×PBS (pH 7.4, 0.22 μm filtered) to make printing solutions at decreasing concentrations from 18 μM to 0.14 μM for BSA conjugates and from 77 μM to 0.6 μM for PVA conjugates. The solutions were transferred into a 384-well plate for printing. We printed microarrays of biotin and DNP conjugates on epoxy-functionalized glass slides (CEL Associates, Pearland, TX) using an OmniGrid 100 contact-printing robot (Genomic Solutions, Ann Arbor, MI) that was equipped with micro-quill printing pins (Majer Precision Engineering, Tempe, AZ). By making the solution-loaded pin contact briefly the glass surface once, approximately 1 nL of the solution was deposited and spread over an area of 130 μm. BSA and amine-modified PVA in the deposited solution bound covalently to the glass surface through the exothermic amine-epoxy reaction.

We fabricated a DNP microarray that consisted of differently loaded DNP-BSA conjugates (5×, 10×, 20× and 40×) and DNP-PVA (0.75% and 1.5%) in titration series, along with unmodified BSA and 10% amine-modified PVA as negative controls. The printed glass slides were stored in a sealed slide box over 24 hours before further processing. Right before an experiment, a printed slide was assembled into a sample cartridge assembly with the printed side immersed in 1×PBS and the opposite side accessible by an OI-RD scanning microscope. The cartridge assembly was connected to a fluid handling system for transferring aqueous solutions to the microarray-bearing surface. The printed surface was soaked in 1×PBS overnight to remove excess printed material including buffer precipitates. Afterward it was washed with a flow of 1×PBS at a rate of 30 mL/min and then exposed to a flow of BSA solution at 7.6 μM in 1×PBS for 10 min before washed again with a flow of 1×PBS for 5 min. The aqueous BSA solution reacted with the remaining free epoxy groups on the printed glass surface, particularly in the unprinted region, thus blocking subsequent protein probes from non-specific reaction with these epoxy groups.

Reactions of anti-DNP goat whole IgG with immobilized DNP-BSA and DNP-PVA conjugates. For protein probes against DNP, we used *unlabeled* goat whole IgG raised against 2,4-dinitrophenol (DNP) purchased from Sigma-Aldrich (St. Louis, MO). The antibody molecules were dissolved in 1×PBS in various concentrations ranging from 57 nM to 452 nM. The experiment was performed on a 60-spot microarray of DNP-BSA conjugates and DNP-PVA conjugates along with BSA and amine-modified PVA as negative controls. Each column corresponds to a distinct conjugate; each row is printed at same concentration. Again after BSA blocking step, the microarray was reacted with a solution of anti-DNP goat whole IgG in 1×PBS at 113 nM for 4 hours. Fig. 3 shows the differential OI-RD image of the microarray after reaction obtained by subtracting the image after BSA blocking from the image taken after the reaction with the microarray still in contact with the probe solution. The results are

qualitatively similar to those of reaction of monovalent F_{ab} fragments of anti-biotin mouse IgG with immobilized biotin-BSA and biotin-PVA conjugates. The anti-DNP goat IgG did not react with printed BSA control as we had expected. Using Eq. (7) in the main article, we converted $\mathrm{Im}\{\Delta_p - \Delta_s\}$ shown in Fig. 3 to the surface mass density Γ of the captured goat whole IgG and display the result in Fig. 4. For comparison, a whole IgG molecule is *Y*-shaped with height of 13 nm (*h*), width of 16 nm (*w*), and thickness of 5 nm (*t*) [1, 2]. If a monolayer of whole IgG consists of closely packed molecules that lay flat on the surface, the surface mass density of such a "side-on" monolayer is $\Gamma_{1\mathrm{ML\ IgG}}^{(\text{side-on})} = t \times \rho_{\text{protein}} = 8.0 \times 10^{-7}\ \mathrm{g/cm^2}$. If instead a monolayer of whole IgG is made of closely packed molecules with F_{ab} domains in contact with the surface while F_c domains pointing away from the surface (upside down *Y*), the surface mass density of such an "end-on" monolayer is roughly $\Gamma_{1\mathrm{ML\ IgG}}^{(\text{end-on})} = h \times \rho_{\text{protein}} = 17.3 \times 10^{-7}\ \mathrm{g/cm^2}$. The surface mass density of the anti-DNP goat IgG molecules captured by DNP-BSA conjugates reaches a plateau near $\Gamma_{1\mathrm{ML\ IgG}}^{(\text{end-on})} = 17.3 \times 10^{-7}\ \mathrm{g/cm^2}$ at around 2.5 μM, now understandably. For 1.5% loaded DNP-PVA (13 kDa) conjugates, the surface mass density of the captured anti-DNP IgG molecules reaches $\Gamma_{1\mathrm{ML\ IgG}}^{(\text{end-on})}$ at close to 5 μM, not far from that for DNA-BSA conjugates. The captured anti-DNP goat whole IgG continue to grow to a surface mass density nearly 3 times $\Gamma_{1\mathrm{ML\ IgG}}^{(\text{end-on})}$, due to an extended target region enabled by the linear structure of a PVA macromolecule. For 0.75% loaded DNP-PVA (13 kDa) conjugates, the surface mass density of the captured anti-DNP goat IgG molecules reaches $\Gamma_{1\mathrm{ML\ IgG}}^{(\text{end-on})}$ at around 15 μM.

Kinetics of anti-DNP goat whole IgG reaction with DNP-BSA and DNP-PVA on glass surface. We repeated the above protein-ligand reactions, but instead of measuring only end-points of the reactions, we followed in real time the amount of the goat IgG captured by the surface-bound conjugates. At t = 0, we replaced 1×PBS buffer in the sample cartridge (0.4 mL

active volume) with an anti-DNP IgG solution at a flow rate of 30 mL/min for a few seconds and then slowed down the flow rate to 0.05 mL/min during the remainder of the reaction. To observe the dissociation of the captured protein probes, we replaced the protein solution with 1×PBS at a flow rate of 30 mL/min for a few seconds and then slowed down the flow rate to 0.05 mL/min during observation. Fig. 5 shows the binding curves for reaction of anti-DNP goat whole IgG with 60 immobilized DNP-BSA and DNP-PBA conjugates. Each panel corresponds to a column in Fig. 5: (a) 40× loaded DNP-BSA; (b) 20× loaded DNP-BSA; (c) 10× loaded DNP-BSA; (d) 5× loaded DNP-BSA; (e) 1.5% loaded DNP-PVA; (f) 0.75% loaded DNP-PVA. The anti-DNP goat whole IgG in 1×PBS at [c] = 113 nM quickly replaced 1×PBS buffer in the sample cartridge at t = 0 and then continued to flow through the cartridge (section 2.3) for 150 minutes. Afterward 1×PBS buffer quickly replaced the IgG solution and continued to flow for another 60 minutes to end the measurement. For DNP-BSA conjugates, the association time was roughly 400 seconds when accessible DNP targets were Moreno more than needed to capture one full end-on monolayer of goat whole IgG; the association time became noticeably longer when the available targets captured more than one full monolayer of the goat IgG. For DNP-PVA conjugates, the association time was roughly 600 seconds when accessible DNP targets were no more than needed to capture one full end-on monolayer of goat whole IgG; the association time became significantly longer (as much as over a factor of 10) when the available targets captured more than one full monolayer of goat IgG. It indicates that with the flexible DNP-PVA conjugates extending into the aqueous ambient, the mass transport though the thick target layer became rate-limiting for the association reaction. Based on these preliminary observations, we performed subsequent measurements of binding kinetics only from printed target spots that captured no more than a full end-on monolayer of protein probes. This minimized the mass transport effect on the measured binding kinetics.

The binding curves of anti-DNP goat whole IgG reactions with 6 DNP-BSA and DNP-PVA

conjugates are displayed in Fig. 6: (a) 40× loaded DNP-BSA; (b) 20× loaded DNP-BSA; (c) 10× loaded DNP-BSA; (d) 5× loaded DNP-BSA; (e) 1.5% loaded DNP-PVA; (f) 0.75% loaded DNP-PVA. Each set consists of the binding curves obtained at 4 probe concentrations: [c] = 452, 226, 113 and 57 nM. The binding curves from the same set were globally fitted using Eq. (5) and (6) (dashed lines in Fig. 6), with the fitting parameters listed in Table 2.

2. Kinetics of drug-specific monoclonal mouse IgG reaction with Digoxin-BSA, Methamphetamine-BSA, Morphine-BSA, Phenobarbital-BSA, Theophylline-BSA and Tetrahydrocannabinol-BSA conjugates immobilized on epoxy-functionalized glass surfaces

Materials. Methamphetamine-BSA (Meth-BSA), Tetrahydrocannabinol-BSA (THC-BSA), and Morphine-BSA (Morph-BSA) were purchased from BIODESIGN International (Saco, ME). Theophylline-BSA (THP-BSA), Phenobarbital-BSA (PB-BSA), and Digoxin-BSA (DIG-BSA) were purchased from Fitzgerald Industries International, Inc. (Concord, MA). Anti-Meth mouse IgG, anti-THC mouse IgG, anti-PB mouse IgG, anti-DIG mouse IgG, and anti-THP mouse IgG were purchased from BIODESIGN International and their equilibrium dissociation constants are not available from the manufacturer. Anti-Morphine mouse IgG molecules were purchased from Fitzgerald Industries International, Inc, and the equilibrium dissociation constant was not available from the manufacturer. These reagents were dissolved in 1×PBS buffer and used without further purification. Since free-form Meth, THC, Morph, THP, DIG, and PB are controlled substances, for our present study we were not able to acquire these drugs to synthesize PVA conjugates.

Microarray of drug-BSA conjugates. We printed six drug-BSA conjugates in duplicates on epoxy-coated glass slides in titration series at printing concentrations of 1 μM, 2 μM, 4 μM, 8 μM, and 16 μM, and unmodified BSA as negative control targets. The drug-BSA conjugate

microarray was washed and BSA-blocked as described in the main text and was in 1×PBS buffer before binding reactions with mouse antibody solutions. The immobilization efficiency of these 6 drug-BSA conjugates was essentially the same as that of biotin-BSA and DNP-BSA conjugates to an epoxy-functionalized glass surface.

Kinetics of drug-specific monoclonal mouse IgG reactions with 6 drug-BSA conjugates immobilized on epoxy-functionalized glass slide surface. To directly obtain the binding kinetics of mouse IgG-drug reactions, we followed in real time the amount of captured mouse anti-drug IgG by the immobilized drug-BSA conjugates printed at concentration of 4 μM. All 6 anti-drug mouse IgG did not react with printed BSA, confirming that the subsequent association-dissociation curves correspond to specific binding of these IgG to their drug targets. At t = 0, we replaced 1×PBS buffer in the sample cartridge (0.4 mL active volume) with an anti-drug mouse IgG solution at a flow rate of 30 mL/min for a few seconds and then slowed down the flow rate to 0.05 mL/min during the remainder of the reaction. To observe the dissociation of the captured protein probes, we replaced the mouse IgG solution with 1×PBS at a flow rate of 30 mL/min for a few seconds and then slowed down the flow rate to 0.05 mL/min during observation. For each drug target, we performed such a real-time association-dissociation experiment at 4 mouse IgG concentrations: [c] = 50 nm, 100 nm, 200 nM, and 400 nM. Fig. 7 shows 6 sets of association-dissociation curves: (a) mouse anti-Digoxin IgG reaction with Digoxin-BSA conjugates; (b) mouse anti-Methamphetamine IgG reaction with Methamphetamine-BSA conjugates; (c) mouse anti-Morphine IgG reaction with Morphine-BSA conjugates; (d) mouse anti-Phenobarbitol IgG reaction with Phenobarbitol-BSA conjugates; (e) mouse anti-Tetrahydrocannabinol (THC) IgG reaction with THC-BSA conjugates; (f) mouse anti-Theophylline IgG reaction with Theophylline-BSA conjugates. The dotted lines are global fits of each set of curves to the two-site Langmuir reaction model (Eq. (5) and (6) in the main article) with $k_{on}^{(1)}$, $k_{off}^{(1)}$, $k_{on}^{(2)}$, $k_{off}^{(2)}$, $N_1^{(0)}/\left(N_1^{(0)}+N_2^{(0)}\right)\equiv\theta^{(1)}$, and $N_2^{(0)}/\left(N_1^{(0)}+N_2^{(0)}\right)\equiv\theta^{(2)}$ as

the fitting parameters. The fitting parameters and the computed equilibrium dissociation constants K_D are listed in Table 3.

The affinity constant of a binding reaction is the inverse of the equilibrium dissociation constant K_D of the same reaction. From Table 2 and Table 3, we find that the affinity constants for 7 anti-drug IgG from 3 different manufacturers to 7 respective drug-BSA conjugates are in the range from 10^9 to 10^{11} M^{-1}. They are comparable in value to the available affinity constants for some of monoclonal mouse anti-drug IgG molecules that Fitzgerald Industries International, Inc. provides commercially (http://www.fitzgerald-fii.com/Products?pId=9&sId=21).

Reference:

(1) Höök, F.; Vörös, J.; Rodahl, M.; Kurrat, R.; Böni, P.; Ramsden, J.J.; Textor, M.; Spencer, N.D.; Tengvall, P.; Gold, J.; Kasemo, B. *Colloid Surf. B: Biointerfaces*, **2002**, *24*, 155-170.

(2) Vörös, J. *Biophys. J.* **2004**, *87*, 553-561.

Table 1. Nitrogen elemental analysis of amine-modified PVA with different chain lengths (molecular weights) and amine loadings. Column 2 shows the expected amine loading; Column 4 shows the actual loadings determined from EA (Column 3).

PVA (kDa)	NaH (equ.)[a]	EA (N%) [b]	NH_2-substitution (x)[c]
2	3%	0.39	1.20%
2	5%	0.52	1.70%
13	1%	0.38	1.20%
13	3%	0.95	3.00%
13	5%	1.78	5.70%
13	10%	2.24	7.10%
89	1%	0.46	1.50%
89	3%	1.10	3.60%

[a] molar percentage of added NaH relative to available hydroxyl groups on PVA;

[b] weight percentage of nitrogen relative to the total molecular weight of the amine-modified PVA from elemental analysis (EA);

[c] molar percentage of NH_2-derivatized hydroxyl groups on the amine-modified PVA relative to initially available hydroxyl groups on PVA computed from the nitrogen content (i.e., column 3).

Table 2: Fitting parameters to measured binding curves for reaction of solution-phase anti-DNP goat whole IgG with surface-immobilized DNP-BSA and DNP-PVA conjugates. The equilibrium dissociation constants $K_D = k_{off}/k_{on}$ are computed from the fitting parameters. Coverage of high-affinity targets are shown in bold face.

	$\theta^{(1)}$	$k_{on}^{(1)}$ $(Ms)^{-1}$	$k_{off}^{(1)}$ $(s)^{-1}$	$K_D^{(1)}$ (nM)	$\theta^{(2)}$	$k_{on}^{(2)}$ $(Ms)^{-1}$	$k_{off}^{(2)}$ $(s)^{-1}$	$K_D^{(2)}$ (nM)
40×BSA	0.58	1.76×10^{3}	1.14×10^{-5}	6.48	**0.42**	2.46×10^{4}	$< 1.4\times10^{-6}$	< 0.057
20×BSA	0.89	1.90×10^{2}	1.64×10^{-5}	86.32	**0.11**	2.75×10^{4}	$< 1.1\times10^{-6}$	< 0.040
10×BSA	0.53	1.23×10^{3}	8.45×10^{-5}	68.70	**0.47**	2.01×10^{4}	$< 1.7\times10^{-6}$	< 0.085
5×BSA	0.42	4.19×10^{3}	7.87×10^{-5}	18.78	**0.58**	4.40×10^{4}	$< 1.7\times10^{-6}$	< 0.039
1.5 % PVA	0.05 [a] 0.05 [b] 0.06 [c] 0.05 [d]	2.34×10^{3}	1.16×10^{-3}	495.7	**0.95** **0.95** **0.94** **0.95**	3.90×10^{3}	$< 3\times10^{-7}$	< 0.077
0.75 % PVA	0.15 [a] 0.26 [b] 0.03 [c] 0.18 [d]	4.60×10^{2}	9.65×10^{-4}	2099	**0.85** **0.74** **0.97** **0.82**	2.21×10^{4}	$< 1.2\times10^{-6}$	< 0.054

[a] [c] = 57 nM. [b] [c] = 113 nM. [c] [c] = 226 nm. [d] [c] = 453 nM.

Table 3: Fitting parameters to measured binding curves for reaction of solution-phase anti-drug mouse monoclonal IgG with 6 commercial drug-BSA conjugates immobilized on epoxy-functionalized glass surface. The equilibrium dissociation constants $K_D = k_{off}/k_{on}$ are computed from the fitting parameters. Coverage of high-affinity targets are shown in bold face.

	$\theta^{(1)}$	$k_{on}^{(1)}$ $(Ms)^{-1}$	$k_{off}^{(1)}$ $(s)^{-1}$	$K_D^{(1)}$ (nM)	$\theta^{(2)}$	$k_{on}^{(2)}$ $(Ms)^{-1}$	$k_{off}^{(2)}$ $(s)^{-1}$	$K_D^{(2)}$ (nM)
Digoxin-BSA	0.82	6.8×10^{3}	3.3×10^{-5}	**4.9**	**0.18**	6.3×10^{4}	1.5×10^{-5}	**0.24**
Methamphetamine-BSA	0.75	4.7×10^{2}	$< 1.1\times10^{-6}$	**< 2.3**	**0.25**	6.5×10^{4}	5.6×10^{-5}	**0.86**
Morphine-BSA	0.20	1.6×10^{3}	$< 1.1\times10^{-5}$	**< 6.9**	**0.80**	4.8×10^{4}	$< 1.1\times10^{-6}$	**< 0.023**
Phenobarbitol-BSA	0.42	1.2×10^{5}	6.2×10^{-5}	**0.53**	**0.58**	6.7×10^{3}	$< 2.8\times10^{-6}$	**< 0.42**
THC-BSA	0.59	2.7×10^{3}	1.9×10^{-5}	**7.1**	**0.41**	3.7×10^{4}	$< 2.3\times10^{-6}$	**< 0.062**
Theophylline-BSA	0.38	2.0×10^{4}	6.8×10^{-6}	**0.34**	**0.62**	8.0×10^{4}	$< 3.9\times10^{-6}$	**< 0.049**

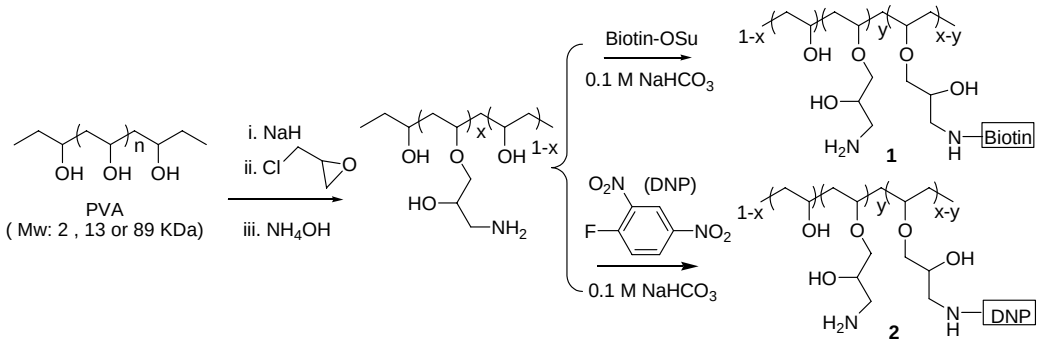

Fig. 1. Chemical steps to derivatize a faction of hydroxyl groups on polyvinyl alcohol (PVA) with primary amine groups and through these amine groups to subsequently conjugate biotin and DNP molecules on amine-modified PVA.

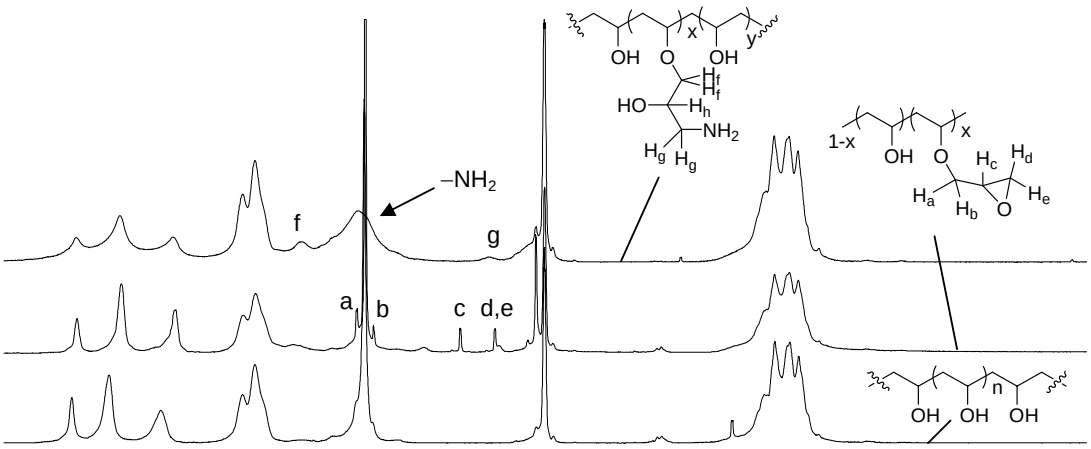

Fig. 2. ^{1}H NMR spectra of unmodified PVA, epoxy-modified PVA, and amine-modified PVA, following the chemical steps that add primary amine groups on PVA. The spectra confirm the high efficiency of the amine conjugation chemistry.

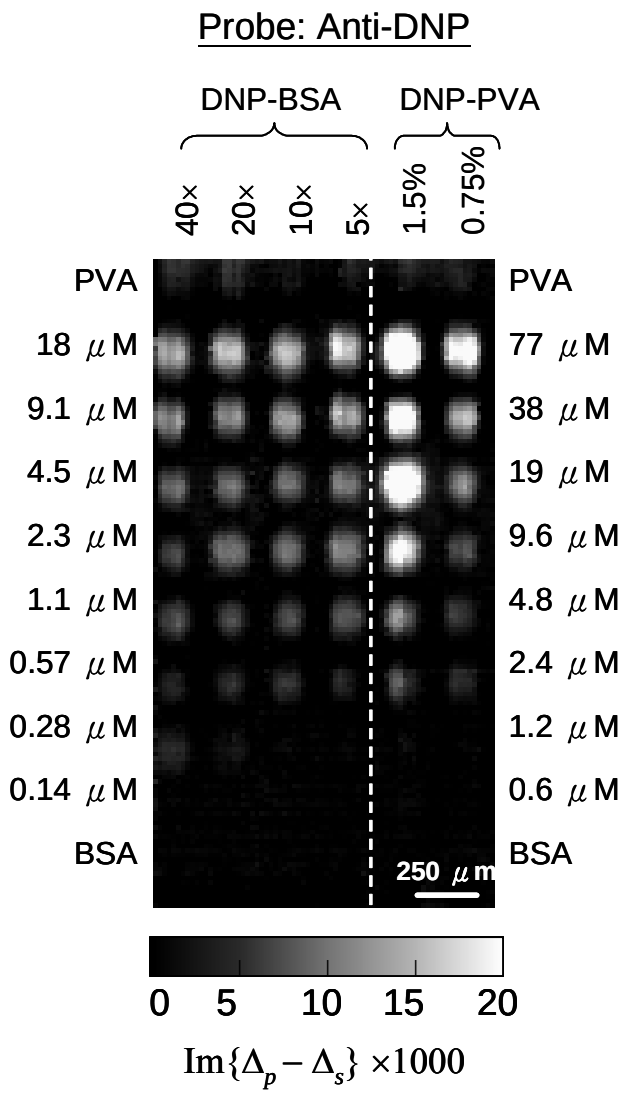

Fig. 3. Differential optical image in $\mathrm{Im}\{\Delta_p - \Delta_s\}$ of a 60-spot DNP-BSA and DNP-PVA conjugate microarray immobilized on an epoxy-coated glass slide after reaction with a solution of anti-DNP goat whole IgG in 1×PBS at 113 nM for 4 hours. The differential image was obtained by subtracting the image taken after BSA-blocking step from the image taken after the subsequent reaction.

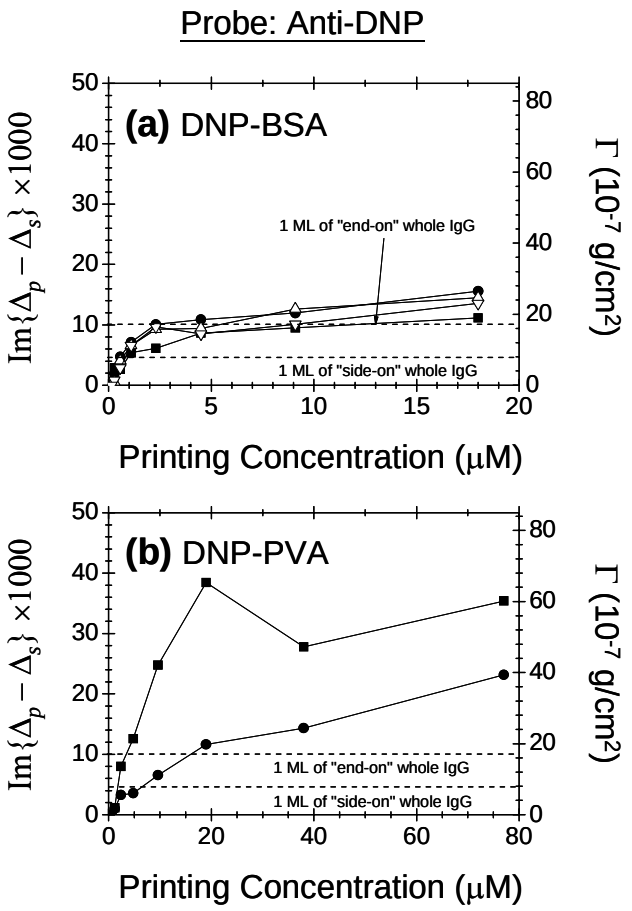

Fig. 4. Change in $\mathrm{Im}\{\Delta_p - \Delta_s\}$ and the corresponding surface mass density (Γ) of anti-DNP goat whole IgG captured by (a) DNP-BSA conjugates, and (b) DNP-PVA conjugates vs. conjugate printing concentration. For DNP-BSA conjugates: (1) solid squares: 40× loading; (2) solid circles: 20× loading; (3) open up-pointing triangles: 10× loading; open down pointing triangles: 5× loading. For DNP-PVA conjugates: (i) solid squares: 1.5% loading; (ii) solid circles: 0.75% loading. Dashed lines are the respective values of a full monolayer of "side-on" and "end-on" goat whole IgG computed using Eq. (7).

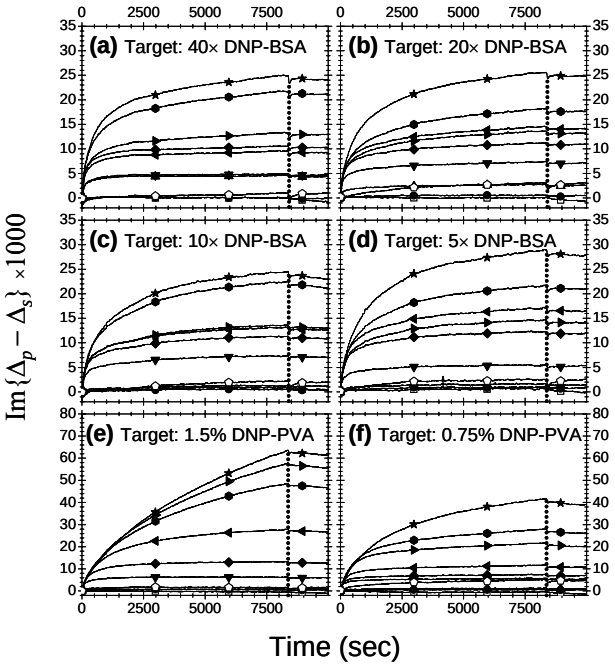

Fig. 5. Simultaneously measured binding curves of anti-DNP goat whole IgG in 1×PBS at 113 nM with 60 DNP targets (see Fig. 7 for layout). Dash lines mark the time when the protein solution is replaced by 1×PBS. Panel (a): 40× loaded DNP-BSA and controls indicated in the first column of Fig. 7; (b) 20× loaded DNP-BSA and controls; (c) 10× loaded DNP-BSA and controls; (d) 5× loaded DNP-BSA and controls; (e) 1.5% loaded DNP-PVA and controls; (f) 0.75% loaded DNP-PVA and controls. For printing concentration of DNP-BSA conjugates: (1) solid stars: 18 μM; (2) solid hexagons: 9.1 μM; (3) solid right-pointing triangles: 4.5 μM; (4) (3) solid left-pointing triangles: 2.3 μM; (5) solid diamonds: 1.1 μM; (6) solid down-pointing triangles: 0.57 μM; (7) solid up-pointing triangles: 0.28 μM; (8) solid circles: 0.14 μM. For printing concentration of DNP-PVA conjugates: (i) solid stars: 77 μM; (ii) solid hexagons: 28 μM; (iii) solid right-pointing triangles: 19 μM; (iv) solid left-pointing triangles: 9.6 μM; (v) solid diamonds: 4.8 μM; (vi) solid down-pointing triangles: 2.4 μM; (vii) solid up-pointing triangles: 1.2 μM; (viii) solid circles: 0.6 μM.

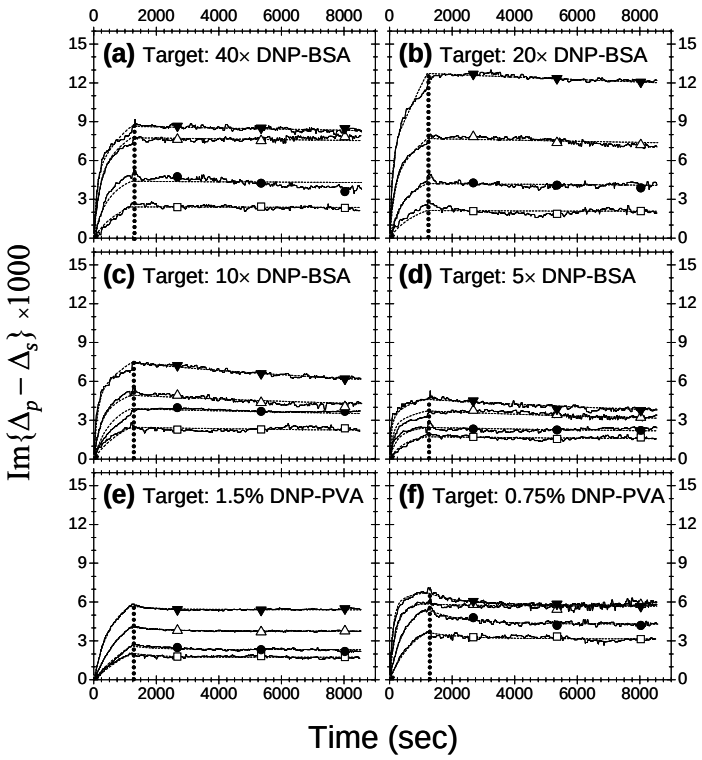

Fig. 6. Simultaneously measured binding curves vs. probe concentration for anti-DNP goat whole IgG reaction with (a) 40× loaded DNP-BSA; (b) 20× loaded DNP-BSA; (c) 10× loaded DNP-BSA; (d) 5× loaded DNP-BSA; (e) 1.5% loaded DNP-PVA; (f) 0.75% loaded DNP-PVA. For probe concentration, (1) open squares: 57 nM; (2) solid circles: 113 nM; (3) open p-pointing triangles: 226 nM; (4) solid down-pointing triangles: 452 nM. The curves in each panel were fitted globally using a two-site Langmuir reaction model (shown in dashed lines). The fitting parameters are listed in Table 2.

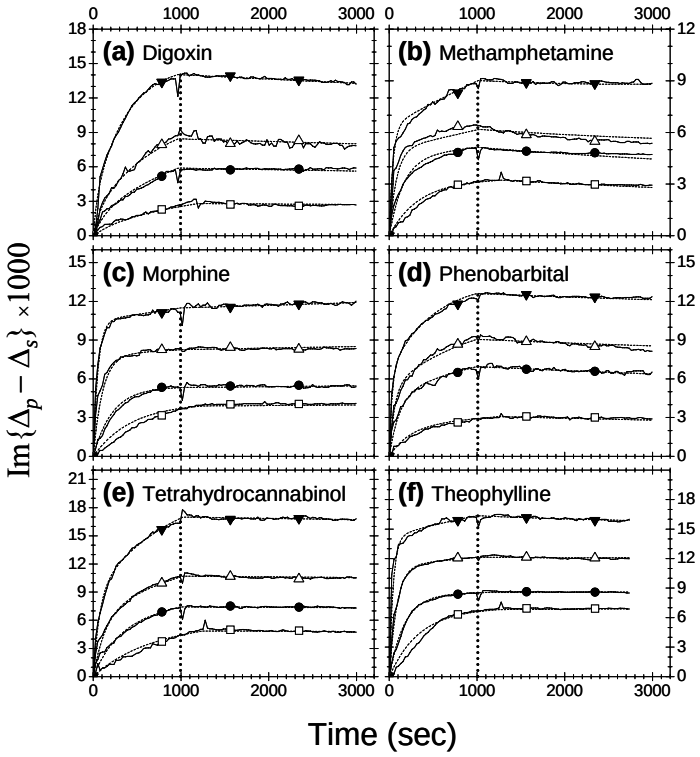

Fig. 7. Association-dissociation curves for monoclonal anti-drug mouse IgG reactions with 6 small-molecule drugs vs. probe concentration (open squares: 50 nM; solid circles: 100 nM; open triangles: 200 nM; solid triangles: 400 nM). The drug molecules were conjugated to BSA and then immobilized on epoxy-functionalized glass surface. Panel (a): Digoxin-BSA. Panel (b): Methamphetamine-BSA. Panel (c): Morphine-BSA. Panel (d): Phenobarbitol-BSA. Panel (e): THC-BSA. Panel (f): Theophylline-BSA. The curves in each panel were fitted globally using a two-site Langmuir reaction model (shown in dashed lines). The fitting parameters are listed in Table 3.